Research Square

Preprints are preliminary reports that have not undergone peer review.
They should not be considered conclusive, used to inform clinical practice,
or referenced by the media as validated information.

Tissue iron enrichment and its links to plant iron accumulation and growth: A meta-analysis of microbial interventions

Qingnan Chu
Institute of Agrifood Research and Technology https://orcid.org/0000-0003-0020-812X
Yuting Zhang
Southwest University
Detian Li
Griffith University
Zhimin Sha
zhiminsha@sjtu.edu.cn

Shanghai Jiao Tong University

Research Article

Keywords: Biofortification, Iron nutrition, Siderophores, Microbial inoculation, Arbuscular mycorrhizal fungi, Plant growth

Posted Date: November 13th, 2026

DOI: https://doi.org/10.21203/rs.3.rs-11714347/v1

License: This work is licensed under a Creative Commons Attribution 4.0 International License.
Read Full License

Additional Declarations: The authors declare no competing interests.

Tissue iron enrichment and its links to plant iron accumulation and growth: A meta-analysis of microbial interventions

Qingnan Chu,[1*] Yuting Zhang,[2] Detian Li,[3] Zhimin Sha[3]*

[1]*Institute of Agrifood Research and Technology (IRTA), Sustainability in Biosystems Programme, Cabrils, 08348, Barcelona, Spain*

[2] *College of Resources and Environment, Southwest University, Chongqing 400715, China*

[3]*Graduate School of Agriculture and Biology, Shanghai Jiaotong University, Shanghai, 200240, China*

*Corresponding author:

Dr. Qingnan Chu

Institute of Agrifood Research and Technology (IRTA), Sustainability in Biosystems Programme, Cabrils, 08348, Barcelona, Spain

Email: qingnan.chu@irta.cat

Prof. Zhimin Sha

School of Agriculture and Biology, Shanghai Jiaotong University, 800 Dongchuan Rd., Shanghai 200240, P.R. China

Email: zhiminsha@sjtu.edu.cn

Abstract

Background and Aims Microorganisms can mobilize iron (Fe), but increased tissue Fe concentration accompanies different growth responses. We quantified tissue enrichment and examined its links with biomass, Fe accumulation and siderophore evidence to assess the nutritional significance of microbial interventions.

Methods We synthesized 533 comparisons from 67 reports and assessed 40 additional comparisons from five reports using missing-SD sensitivity analyses. Multilevel models separated tissue Fe concentration, Fe amount and soil Fe. Within-experiment matching aligned organs and paired directly measured Fe concentration with organ dry mass.

Results Across 181 comparable concentration comparisons from 34 study clusters, inoculation increased tissue Fe concentration by 14.6% (95% confidence interval 6.2–23.7%). The 95% prediction interval ranged from −33.1% to +96.3%. Among 58 concentration–dry-mass pairs from 16 reports, both means increased by more than 5% in 25 comparisons from 11 reports, representing 46.8% of the study-balanced distribution (95% interval 27.1–66.5%). Seven comparisons from four reports combined greater dry mass with lower Fe concentration. Formal tests did not identify a consistent organ or microbial-group advantage. Field evidence comprised 22 comparisons, and only three reports tested targeted siderophore loss. Only one report quantified grain Fe amount, highlighting limited evidence for harvested-organ nutritional output.

Conclusion Microbial inoculation increases tissue Fe concentration on average, and enrichment coincides with greater biomass. Their variable alignment supports joint assessment of concentration, organ dry mass and Fe accumulation. This synthesis provides a framework for distinguishing tissue enrichment from coordinated nutritional and growth benefits when evaluating microbial contributions to plant Fe nutrition.

Keywords: Biofortification; Iron nutrition; Siderophores; Microbial inoculation; Arbuscular mycorrhizal fungi; Plant growth

Abbreviations: AMF, arbuscular mycorrhizal fungi; BH, Benjamini–Hochberg; CI, confidence interval; CR2, small-sample cluster-robust variance estimator; DW, dry weight; DTPA, diethylenetriaminepentaacetic acid; Fe, iron; lnRR, log response ratio; REML, restricted maximum likelihood

Introduction

Iron (Fe) is abundant in most soils, yet only a small fraction is readily available for plant uptake (Marschner 2011). This discrepancy is particularly pronounced in alkaline and calcareous soils, where high pH and the low solubility of Fe(III) compounds severely restrict Fe availability, often resulting in Fe deficiency and chlorosis despite substantial total soil Fe reserves (Lindsay and Schwab 1982; Colombo et al. 2014; Malisic et al. 2026). As an essential micronutrient, Fe participates in photosynthesis, respiration and numerous electron-transfer processes, making its acquisition and homeostasis critical for plant growth (Hänsch and Mendel 2009; Kobayashi and Nishizawa 2012; Briat et al. 2015; Chu et al. 2019). Fe availability in the rhizosphere is regulated by complex interactions among soil pH, redox conditions, organic ligands and biological activities. Plant roots and associated microorganisms can modify these conditions through acidification, Fe reduction and the release of Fe-binding compounds, potentially improving Fe mobilization and acquisition (Lemanceau et al. 2009; Marschner 2011; Colombo et al. 2014). However, whether such rhizosphere-mediated changes translate into greater Fe accumulation and improved plant growth remains an important question.

Plants employ distinct strategies for Fe acquisition and differ in how Fe is transported and distributed after uptake (Kobayashi and Nishizawa 2012; Connorton et al. 2017; Chu et al. 2026). Following uptake, Fe must be redistributed through coordinated transport, chelation and intracellular allocation processes, including emerging chaperone-mediated pathways (Chu 2026). Most non-grass plants acquire Fe primarily through rhizosphere acidification, ferric-chelate reduction and subsequent Fe(II) uptake (Strategy I), whereas grasses generally release phytosiderophores to mobilize Fe(III) and take up Fe(III)–phytosiderophore complexes (Strategy II). Rice additionally possesses an Fe(II) uptake pathway, illustrating the physiological diversity of Fe acquisition even within grasses (Ishimaru et al. 2006; Connorton et al. 2017). Beyond these plant-derived mechanisms, microbial siderophores can influence Fe mobilization and, under certain conditions, provide additional routes for plant Fe acquisition (Schalk 2025; Gu et al. 2026a). However, the accessibility of siderophore-bound Fe varies with ligand chemistry and plant species. For example, barley preferentially acquired Fe from a phytosiderophore rather than the microbial chelates tested by (Römheld and Marschner 1986), whereas microbial-siderophore-derived Fe uptake was demonstrated in oat under defined experimental conditions (Crowley et al. 1988). Therefore, microbial Fe mobilization, plant Fe acquisitioin and

subsequent internal Fe distribution represent distinct processes that should not be assumed to produce equivalent nutritional outcomes.

Microorganisms influence this supply through several routes. Siderophores bind Fe and support microbial acquisition, potentially mobilizing mineral Fe while also strengthening microbial competition (Crowley et al. 1991; Schalk 2025). Other microbial activities change root development, host signalling, rhizosphere acidification and nutrient exploration; arbuscular mycorrhizal fungi (AMF) provide a distinct symbiotic route for nutrient acquisition (Singh et al. 2025). In red clover, rhizobial inoculation enhanced Fe acquisition together with root ferric-reduction responses even though the tested rhizobia lacked a detectable siderophore signal under the assay conditions (Jin et al. 2006). Recent reviews integrate microbial siderophores into plant Fe nutrition and rhizosphere functioning, emphasizing the variety of possible routes and interactions (Gu et al. 2026a, b). Identifying which route explains a treatment response remains central to interpreting microbial effects.

The endpoint measured is equally important. Fe concentration expresses Fe relative to tissue mass, whereas Fe amount describes the accumulated pool in an organ or plant. For compatible measurements, Fe amount equals concentration multiplied by dry mass. Growth can therefore dilute Fe concentration despite increased accumulation, while growth suppression can raise concentration without increasing the accumulated pool (Jarrell and Beverly 1981). Roots add a spatial distinction: measured Fe may be surface associated, apoplastic or intracellular, and these pools are not necessarily equivalent in their contribution to plant Fe nutrition (Bienfait et al. 1985). Apoplastic Fe reserves can contribute to shoot supply, with their mobilization depending on Fe status and source (Bienfait et al. 1985; Zhang et al. 1991). Soil diethylenetriaminepentaacetic acid (DTPA) extraction, in turn, measures an operationally defined chemical pool of potentially available Fe rather than Fe uptake itself (Lindsay and Norvell 1978). Connecting these measurements with organ Fe amounts and biomass is therefore necessary to evaluate whether apparent improvements in Fe availability or tissue concentration translate into meaningful nutritional benefits.

Previous syntheses established the value of considering nutrient identity, tissue and growth together. Lehmann and Rillig (2015) examined AMF effects on Cu, Mn and Fe concentrations, tissue and environmental variation, nutrient amounts and biomass, while correcting shared-control dependence. Zhang et al. (2023) synthesized growth responses to siderophore-producing bacteria, and Yang et al. (2026) examined microbial effects across essential and toxic metals alongside biomass and

physiology. These studies motivate a more explicitly matched question: do root and shoot Fe responses differ under the same experimental conditions, and do Fe-amount gains accompany or exceed growth in the same organ? A second question concerns attribution: how closely does the siderophore evidence apply to the treatment whose Fe response is synthesized?

We addressed these questions through a unified multilevel synthesis of comparable tissue Fe concentrations, separate analyses of Fe amount and soil Fe, and condition-matched organ and growth contrasts. The unified model formally compared bacteria, AMF and other fungi across roots, shoots and leaves, while preserving the distinction between microbial inoculation and siderophore preparations with different comparators. Matched responses then connected concentration changes with organ Fe pools and dry biomass. Finally, report- and treatment-level evidence classifications distinguished a microbial Fe response from a demonstrated siderophore contribution. This combined framework evaluates the consistency of tissue enrichment and the experimental links that support its interpretation as improved plant Fe nutrition.

Materials and methods

Review scope and information sources

We synthesized plant Fe responses to microbial interventions and evaluated their links with growth and siderophore evidence, following PRISMA 2020 and PRISMA-S reporting principles (Page et al. 2021; Rethlefsen et al. 2021). Supplementary Information (**Online Resource 1**, PDF) contains the search strategies, supplementary methods, figures, tables and the complete reference list of included reports. Supplementary Data (**Online Resource 2**, Excel) contains extracted group summaries, experimental identifiers and report decisions.

Scopus and AGRIS were searched on 3 November 2026, USDA National Agricultural Library on 4 November, and PubMed on 3 November with the same query updated and reconciled on 8 November. Queries combined plant/rhizosphere, microbial/mycorrhizal/siderophore and Fe nutrition/acquisition/availability terms, without deliberate year or language restrictions. Citation searching, local collections and relevant review reference lists supplied additional reports. Google Scholar supported supplementary discovery. Completed database exports did not include CNKI, Web of Science or CAB Abstracts.

DOIs, PubMed identifiers and normalized titles supported deduplication and companion-report checks. Database-matched reports were assigned to the database branch; remaining retrieval targets entered the other-methods branch. Unobtainable reports were recorded separately as not retrieved.

Eligibility and source verification

Eligible comparisons required a plant experiment, a microbial or siderophore-containing intervention, a compatible comparator, a directly measured target Fe outcome and positive treatment and control means. The dataset with reported uncertainty additionally required an interpretable SD or SE and an identifiable independent n. Target outcomes were total tissue Fe concentration, directly reported organ/plant Fe amount, DTPA-extractable soil Fe and soluble soil Fe. Organs, mass bases and assays were retained separately. Active Fe, isotope-specific measurements and semiquantitative signals remained outside these pooled endpoints.

Interventions distinguished bacteria, AMF, other fungi/yeasts, mixed inocula and siderophore preparations. Estimands distinguished inoculation against a matched uninoculated control, addition to an existing microbial partner, equal-Fe source replacement and siderophore addition at the same Fe supply. Preparations supplying extra Fe were coded separately. Fe amount denotes a harvested pool. Dry mass was the growth endpoint.

We extracted means, error values and definitions, independent n, units, organs, treatments, backgrounds and numerical source locations. Pots, plots, containers or biological pools defined n; analytical subsamples did not add replication. SE was converted as SD = SE × $\sqrt{n}$. Numerical tables and source data were preferred; calibrated graph coordinates retained their source and precision notes. We did not reconstruct Fe-amount uncertainty from separately published concentration and biomass means.

This study compiled data from 67 published reports, comprising 533 comparisons with reported uncertainty. An additional 40 comparisons from five reports lacking uncertainty estimates were included in the CV sensitivity analysis. The extracted data were systematically organized, coded and analyzed to evaluate the effects of microbial interventions on plant Fe concentration, Fe accumulation and growth.

Experimental context and evidence classification

Culture medium and experimental setting were coded separately. Media distinguished soil/substrate, solution/gel and sand/perlite supplied with nutrient solution; setting distinguished field and controlled experiments. Fe environment and host categories used source descriptions, preserving source-soil pH as a proxy when experimental pH was unavailable. Publication years followed original publication or thesis dates rather than later platform upload dates.

Seven reporting domains covered allocation, experimental units, matched treatment–control background, missing samples, measurement blinding, numerical source and selective outcome reporting. Root-cleaning descriptions were assigned only to the relevant mineral-analysis experiment. Siderophore categories distinguished no direct test, trait/potential, crude material, isolated/defined material, targeted functional loss, and targeted loss with specific rescue of the plant Fe outcome. These describe evidence types rather than a summed causal score. Report-level tests were attributed to individual comparisons only when the treatment and outcome matched. The evidence and quality profile covers the 67 reports with reported uncertainty; the five CV-only reports form a separate sensitivity extension.

Effect sizes and unified concentration models

Effect size was quantified as the natural-log response ratio (lnRR):

$$Effect\ size = LnRR = Ln(\frac{X_t}{X_c}) \quad (1)$$

where X_t and X_c are the mean values of the treatment and control, respectively.

For outcomes reported on the raw (arithmetic) scale, the sampling variance (v) of lnRR was calculated as:

$$\mathrm{v} = \frac{s_t^2}{n_t X_t^2} + \frac{s_c^2}{n_c X_c^2} \quad (2)$$

where S_t and S_c are the standard deviations, and n_t and n_c are replicate number for treatment and control groups, respectively. When SE was reported, SD was obtained as SE × $\sqrt{n}$; when 95% CI were reported, the corresponding SD was back-calculated.

Adjudicated blocked or paired comparisons retained their covariance adjustment; shared-arm covariance entered the sampling covariance matrix (Lajeunesse 2011). Restricted maximum likelihood (REML) models included study-cluster and within-study effect random intercepts. Small-sample

cluster-robust variance estimator (CR2) standard errors and Satterthwaite or approximate Hotelling T^2 inference accounted for study-cluster dependence (Tipton 2015). Estimates were transformed as $100 \times [exp(ln\, RR) - 1]$.

The unified target comprised dry-weight total Fe concentrations following bacteria, AMF or other-fungal inoculation versus a matched uninoculated control. The three-organ model used roots, shoots and separately sampled leaves. We fitted additive intervention + organ and intervention × organ models, and calculated a marginal mean giving equal weight to each of the nine observed intervention–organ cells. Thus, heavily sampled organs or microbial groups did not define the target average. Joint tests formally evaluated intervention, organ and interaction terms; pairwise contrasts were Benjamini–Hochberg (BH)-adjusted within comparison families. All-organ models included the other reported tissue categories as an extension. This standardizes the target to a balanced microbial-group and organ mix instead of letting the most frequently sampled cells determine it. An intercept-only multilevel REML model on the identical 181 comparisons provided a conventional inverse-marginal-covariance-weighted overall estimate as a sensitivity check.

Fe amounts, soil Fe and preparations with different estimands were analyzed in separate outcome-specific strata requiring at least three study clusters. Eighteen strata were estimable within a previously specified 19-test family; BH adjustment retained the non-estimable hypothesis (Benjamini and Hochberg 1995). Confidence intervals were unadjusted, with q values reported separately. Technical covariance stabilization, heterogeneity estimation and handling low degrees of freedom (df) are detailed in Online Resource 1. We report study-level and effect-level residual variance components on the lnRR scale. An approximate 95% prediction interval for a new true effect at the standardized fixed-effect target was calculated using the t critical value based on CR2-adjusted Satterthwaite degree of freedom and the square root of the sum of the marginal-mean variance and the two estimated residual variance components.

Diagnostics and missing-SD sensitivity

Unified moderator models evaluated medium and field/controlled setting. Within-stratum Fe-environment and host summaries remained exploratory. Small-study diagnostics used $\sqrt{\frac{1}{nt} + \frac{1}{nc}}$, where n_t and n_c represent the sample sizes of the treatment and control groups, respectively. Models

were adjusted for intervention and organ to avoid using an lnRR-derived SE as the predictor (Nakagawa et al. 2022). Publication year was centred at 2010 and scaled per decade; both predictors were also fitted jointly. These evaluate sample-size association and publication-year trends, rather than actual publication delay.

We audited the original 287 broad numerical/design exclusions into source-supported reasons and reopened comparisons for CV sensitivity only when positive arm means, exact independent n, compatible outcomes and matching controls were traceable. Forty comparisons from five reports qualified. Missing means, n and incompatible designs were not repaired. This extension covers verified stored comparisons and does not exhaust all potentially recoverable mean-only tables in the excluded literature.

CV donors came from the same endpoint and, where at least five reports were available, the same organ. Shared arms were deduplicated. CVs were n-weighted within reports and weighted by mean arm n across reports. Imputed SD equalled donor CV × arm mean; known SDs were unchanged and shared-arm covariance was retained. We used 2,000 report-bootstrap draws to define low, central and high donor-CV scenarios. This implements a study-balanced CV sensitivity motivated by (Nakagawa et al. 2023); the scenarios do not fully propagate imputation uncertainty.

Additional sensitivities varied unknown within-study correlations, graph inclusion, specific numerical concerns, reporting domains and a small-sample lnRR correction (Lajeunesse 2015). The unified model used unknown-correlation scenarios of 0.3 and 0.6; earlier stratum-specific sensitivities retained their original settings. Leave-one-cluster-out analyses and study-mean summaries assessed influence. CV-extended outcome strata retained the original 19-test adjustment family.

Matched organ and growth responses

Effects were matched within report, cohort, host, treatment, control, time, organ definitions, mass basis and assay. The organ contrast was $\Delta\text{organ} = \text{lnRR}_{\text{root}} - \text{lnRR}_{\text{upper}}$, with variance $v_{\text{root}} + v_{\text{upper}} - 2\text{cov}(\text{root, upper})$. Root–shoot and root–leaf matches remained separate. Arm-level covariance and a reference cross-organ correlation of 0.5 supported multilevel CR2 models; correlation sensitivities and the separate three-test adjustment are described in Online Resource 1. This is a difference in relative organ responses, rather than a transport flux.

Fe-amount and dry-mass responses were matched within the same organ and condition. Δgrowth

= $\ln RR_{Fe\ amount} - \ln RR_{DW}$ describes their relative response ratios. With unavailable cross-outcome covariance, the principal exploratory summary averaged responses within study and stratum, then used equal-study means and t intervals. Three eligible contrasts formed a separate BH family. Variance-weighted ordinary and modified Hartung–Knapp analyses assessed sensitivity (Röver et al. 2015). Descriptive joint-response counts used ±5%, with 0% and 10% sensitivity bands. Soil–plant links retained their assay and endpoint identities and were summarized descriptively. Analyses used R 4.6.1, metafor 5.2-1 and clubSandwich 0.7.0 (Viechtbauer 2010).

Directly measured Fe concentration was paired with organ dry mass for the same treatment contrast, background and harvest. Fresh mass, whole-plant mass for a sampled organ, medians and unmatched factorial means were excluded. Mean responses were classified using a ±5% band, with direction-only and ±10% classifications as sensitivities. We calculated joint-response proportions within each study and averaged them with equal study weights; 95% percentile intervals used 20,000 study-cluster bootstrap resamples (seed 20261109). These describe the distribution of mean responses, with a separate analysis restricted to pairs with complete uncertainty information (**Online Resource 1, Fig. S4**).

Exploratory context models

Context models added one focal moderator to the established microbial-class and organ model; duration models also adjusted cultivation medium and used $\log_2$ days. We assessed independent-study coverage, category overlap, model rank and focal CR2 degrees of freedom before interpretation. Practical feasibility guides were at least ten study clusters and focal df of at least four, with df below ten indicating limited precision. Tests of duration, host strategy and target composition were exploratory; their nominal *P* values and a separate three-test BH sensitivity are reported together in **Table S2**. Low-coverage or confounded variables were summarized as evidence coverage. Covariance and source-definition sensitivities are described in **Online Resource 1**.

Results

The quantitative corpus spans tissue enrichment and fewer matched nutritional endpoints

The review included 72 reports contributing 573 source comparisons: 67 reports supplied 533

256 comparisons with reported sampling uncertainty, and five additional reports supplied 40 comparisons
257 used only in CV sensitivities (**Fig. 1; Table 1**). The dataset with reported uncertainty comprised 375
258 tissue Fe concentrations, 120 organ or plant Fe amounts, 35 DTPA-extractable soil Fe measurements
259 and three soluble-soil-Fe measurements. Its 55 concentration, 19 Fe-amount and five soil-Fe reports
260 overlapped across outcomes. The CV extension added 16 concentration and 24 Fe-amount
261 comparisons.

262 **Table 1. Coverage of Fe outcomes in the reported-uncertainty dataset and CV-only extension**

Outcome	Reports with uncertainty	Comparisons with uncertainty	CV-only reports	CV-only comparisons
Tissue Fe concentration	55	375	3	16
Organ or plant Fe amount	19	120	3	24
DTPA-extractable soil Fe	5	35	0	0
Soluble soil Fe	1	3	0	0
Distinct total	67	533	5	40

263 Reports can contribute to more than one outcome. The combined quantitative corpus contains 72 distinct reports
264 and 573 source comparisons. CV-only comparisons retain missing source SDs in **Online Resource 2**.

265 From 10,150 saved database entries, 3,122 duplicates were removed and 7,028 records screened.
266 Database screening led to 266 retrieval targets and 265 obtained reports; other methods contributed
267 134 targets and 119 obtained reports. Of 384 full texts assessed, 72 entered at least one quantitative
268 analysis and 312 were excluded; 16 retrieval targets remained unavailable (**Fig. 1**). The original 287
269 numerical/design exclusions yielded five CV-only reports and 282 remaining exclusions. Source-
270 specific reasons and the other 30 full-text exclusions are retained in **Online Resource 2**.

271 Field evidence comprised 22 comparisons with reported uncertainty from six reports; 511
272 comparisons came from controlled experiments. The field subset mixed organs, endpoints and
273 interventions. Grain or kernel Fe amount was reported in two eligible comparisons from one report;
274 no compatible root–grain pair or grain Fe amount–dry-mass pair qualified for the matched analyses.

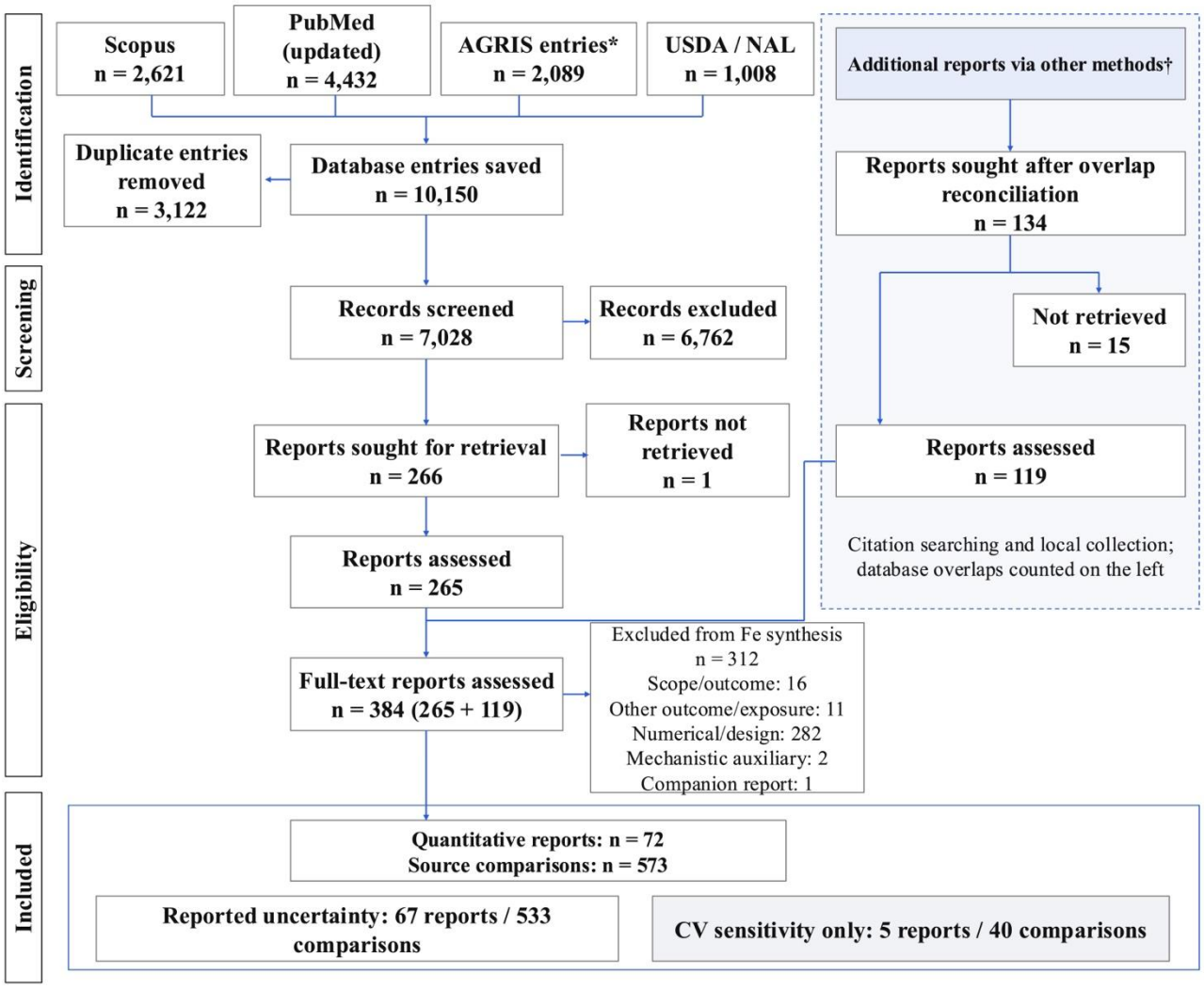


Fig. 1 PRISMA flow diagram of study identification, screening and inclusion. Database counts refer to exported metadata records after reconciliation of AGRIS versions. Full-text eligibility decisions are provided in Supplementary Data (**Online Resource 2**), and references for all included reports are listed in the Appendix of Supplementary Information (**Online Resource 1**). CV: coefficient of variation.

Inoculation increased tissue Fe concentration across the comparable evidence base

The unified three-organ dataset comprised 181 comparisons from 34 study clusters. Its standardized marginal response was +14.6% (95% CI 6.2–23.7%; $P = 0.001$) in the additive model and +13.8% (95% CI 5.1–23.2%; $P = 0.0035$) in the interaction model (**Fig. 2a**). Adjusted marginal estimates across organs were +17.2% for bacteria (95% CI 1.4–35.5%), +8.1% for AMF (−6.3–24.7%) and +18.8% for other fungi (−0.2–41.5%; **Fig. 2b**). Residual study-level and effect-level variances were 0.0336 and 0.0342 $\ln RR^2$, respectively. The approximate 95% prediction interval was −33.1 to +96.3%. The conventional intercept-only estimate was +13.8% (95% CI 5.9–22.2%; the same 181

comparisons and 34 clusters).

Formal joint tests yielded $P = 0.652$ for microbial group and $P = 0.518$ for organ in the additive model. The interaction test yielded $P = 0.582$, with a denominator df of 2.86. The marginal positive response therefore coexisted with limited precision for differences among groups and organs. The all-organ extension comprised 248 comparisons from 40 study clusters.

Outcome-specific stratification retained the positive bacterial root-concentration estimate of +24.8% (95% CI 12.7–38.3%; seven clusters, 21 comparisons; $q = 0.043$). Bacterial shoot and leaf estimates were +22.8% and +34.2%, respectively, with broader intervals and $q > 0.05$ (**Online Resource 1, Fig. S1**). These separate-stratum estimates use stratum-specific heterogeneity and complement the formal contrasts from the unified model.

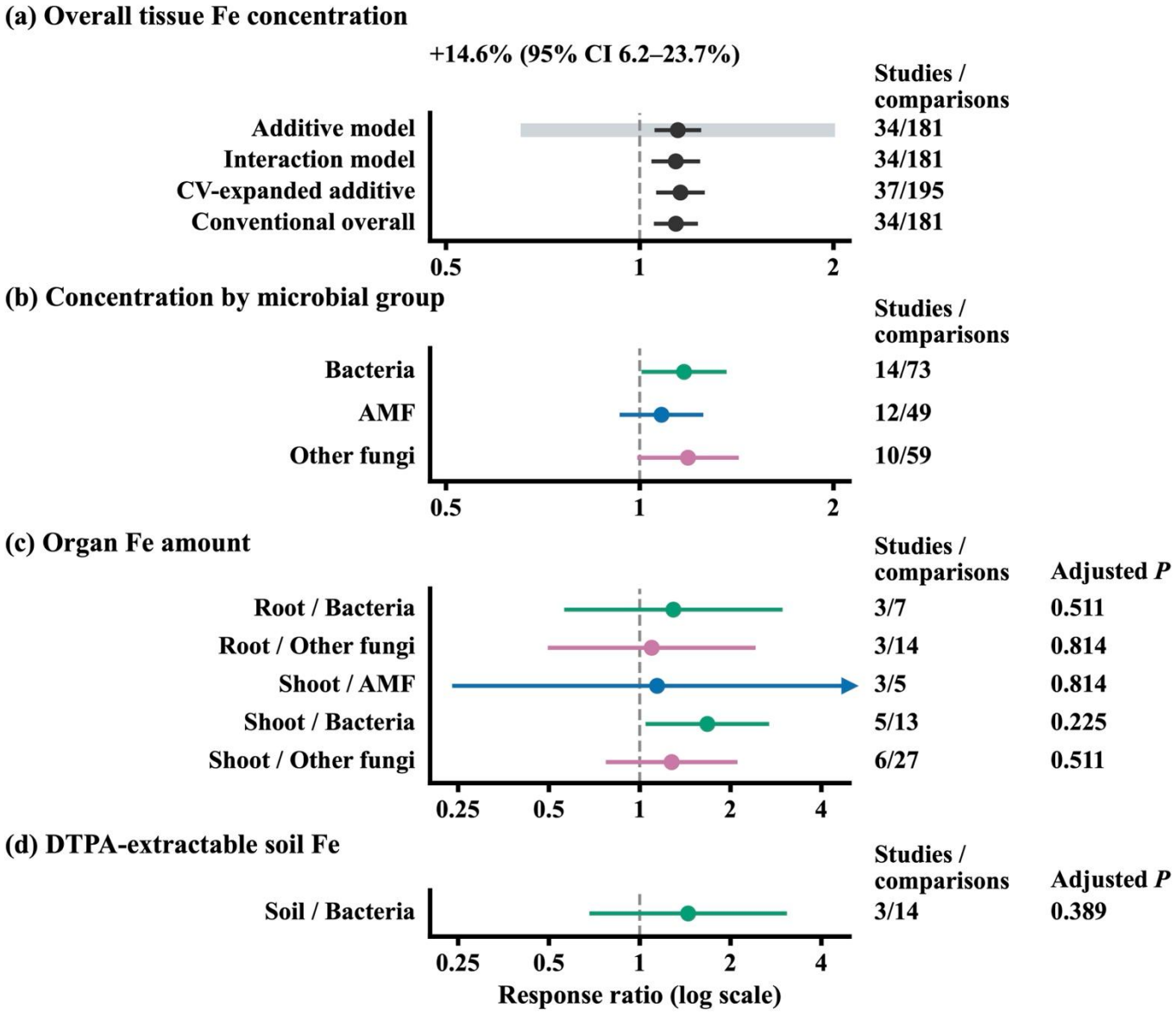


Fig 2. Microbial effects on tissue Fe concentration, Fe amount and DTPA-extractable soil Fe. (a) Standardized marginal concentration responses from the original additive and interaction models (181 comparisons, 34 study clusters) and the CV-expanded additive model (195 comparisons, 37 clusters). All give equal weight to the nine bacteria/AMF/other-fungi by root/shoot/leaf cells. (b) Intervention-specific marginal means across the three organs from the additive model. Group differences were tested jointly (P = 0.652); (c) Separate outcome-specific Fe-amount models and (d) bacterial DTPA-extractable soil Fe. Points and lines show estimates and unadjusted 95% study-cluster CR2 confidence intervals. Studies/comparisons gives the numbers of independent study clusters and treatment–control comparisons. Adjusted P values in (c) and (d) use the Benjamini–Hochberg procedure across 19 outcome-specific tests. The pale bar in (a) shows the 95% prediction interval; arrows indicate intervals extending beyond the plotting range.

Fe-amount responses were positive on average but less precisely resolved

Bacterial inoculation increased shoot Fe amount by an estimated 67.6% (95% CI 6.2–164.5%; five clusters, 13 comparisons; q = 0.225), while the root estimate was +29.3% (−42.9–193.0%; three clusters, seven comparisons). Shoot Fe-amount estimates were +14.2% for AMF (−75.7–437.2%; three clusters, five comparisons) and +27.6% for other fungi (−21.6–107.6%; six clusters, 27 comparisons). None of the five estimable Fe-amount strata retained support in the original 19-test family (**Fig. 2c**).

The bacterial DTPA-extractable soil-Fe estimate was +44.7% (95% CI −30.8–202.9%; three clusters, 14 comparisons; q = 0.389; **Fig. 2d**).

Matched responses provided no clear evidence of preferential root enrichment

Strict matching yielded 83 root–upper-organ pairs from 19 reports: 66 root–shoot and 17 root–leaf pairs. Three estimable strata covered 28 contrasts from eight distinct reports. Root-relative-to-shoot concentration responses were −3.9% for bacteria (95% CI −18.3–13.0%; four clusters, 11 pairs; q = 0.462) and +6.0% for other fungi (−28.5–57.1%; three clusters, 10 pairs; q = 0.462). The bacterial Fe-amount difference was −18.9% (−41.5–12.4%; three clusters, seven pairs; q = 0.294; **Fig. 3a**).

Among the seven bacterial root-concentration reports, three described ordinary water washing and four did not explicitly describe washing for the relevant experiment. None validated root-surface Fe removal in that experiment. Same-condition shoot Fe amount was available for two cultivar contrasts in one report; these were not accompanied by a demonstrated parallel growth gain.

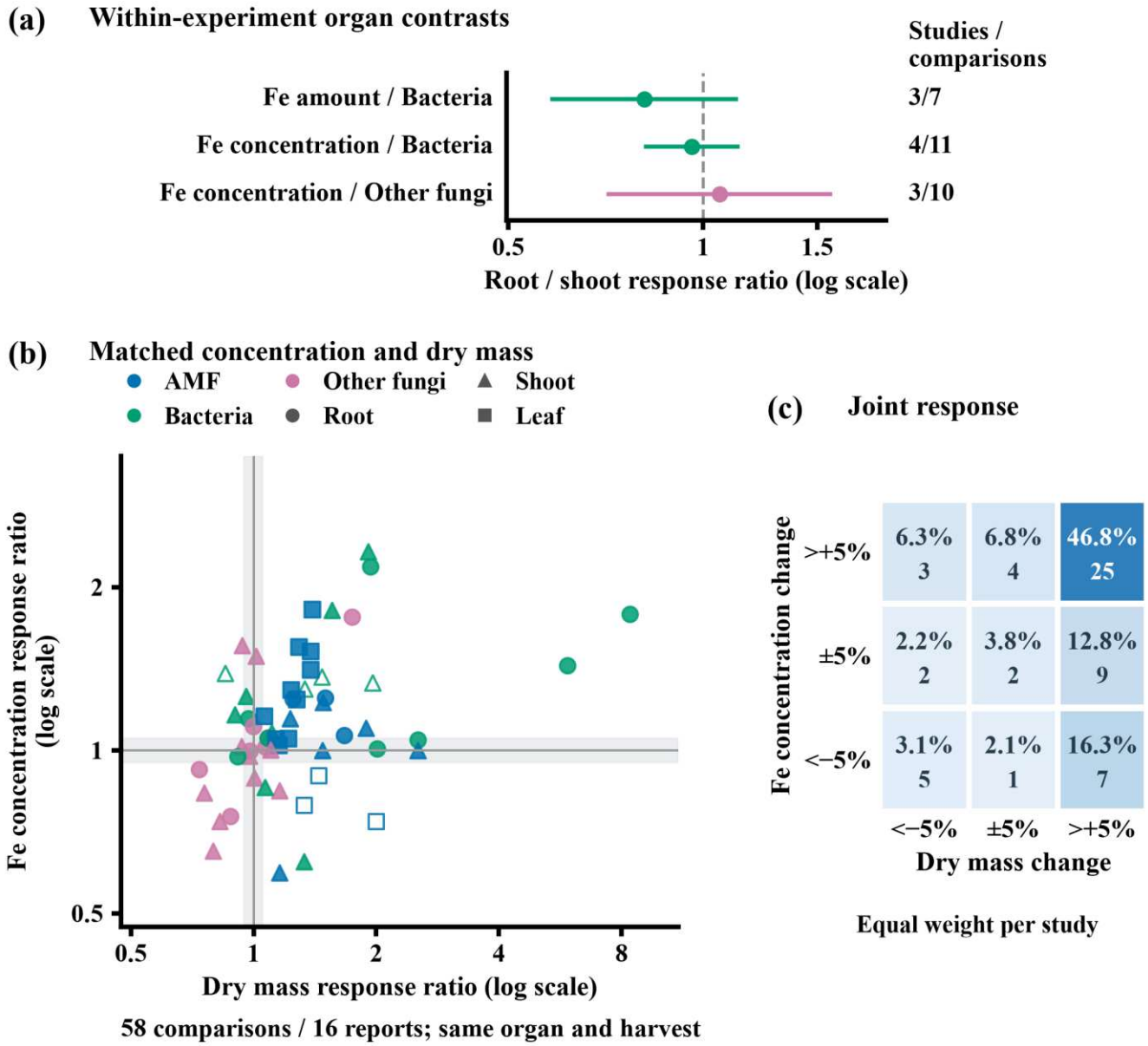


Fig. 3 Matched organ contrasts and joint Fe concentration–growth responses. Intervals in (a) are unadjusted 95% study-cluster CR2 confidence intervals; counts indicate independent study clusters/treatment–control comparisons. In (b), shading marks the ±5% band and open symbols identify pairs with unresolved or rounded uncertainty. Cells in (c) show study-balanced percentages above comparison counts, with equal total weight per study. Categories describe mean responses. The panels use bacterial, AMF and other-fungal inoculation against matched uninoculated controls; Fe amount–dry-mass pairs are shown separately in **Online Resource 1, Fig. S3**

Direct tissue enrichment often coincided with increased organ biomass

Directly measured Fe concentration and dry mass were matched for 58 comparisons from 16 reports: 27 shoot, 18 root and 13 leaf comparisons (**Fig. 3b,c**). Both means increased by more than 5% in 25 comparisons from 11 reports. This was the most frequent joint-response category, accounting for

46.8% of the study-balanced distribution (95% study-cluster bootstrap interval 27.1–66.5%). Seven comparisons from four reports combined increased dry mass with lower Fe concentration (16.3%), and three comparisons from three reports combined increased concentration with lower dry mass (6.3%). Nine further comparisons showed increased dry mass with Fe concentration remaining within ±5% of the control (12.8%). Restriction to 51 comparisons from 14 reports with complete uncertainty information yielded a similar joint-increase proportion of 48.1% (27.5–69.4%). Joint increases represented 59.4% under direction-only classification and 33.8% with a ±10% band (**Online Resource 1, Fig. S4**).

The complementary Fe amount–dry-mass dataset contained 72 variance-complete pairs from 12 reports. 24 comparisons increased by more than 5% in both outcomes, and 16 decreased in both. Among 47 live-inoculation pairs from nine study clusters, the Fe-amount versus dry-mass slope was 1.06 (95% CI 0.47–1.66; $P = 0.007$); the all-pair slope was 0.87 (0.57–1.17). These associations are shown separately in **Online Resource 1, Fig. S3**.

Table 2. Matched shoot Fe amount and dry-mass responses shown as percent change (95% CI)

Intervention	Reports	Pairs	Fe amount	Dry mass (DW)	Relative Fe / DW	*q*
AMF	3	5	11.1 (-54.2, 169.6)	7.9 (-13.7, 34.9)	3.0 (-52.0, 120.9)	0.884
Bacteria	3	6	41.7 (-14.2, 134.2)	7.7 (-25.2, 55.1)	31.6 (1.9, 70.1)	0.132
Other fungi	3	9	9.0 (-53.8, 157.1)	16.4 (-58.1, 223.4)	-6.4 (-51.3, 80.1)	0.884

Equal-study summaries use t intervals (df = 2). q adjusts the three growth-difference tests. Relative Fe / DW is the Fe-amount response ratio divided by the dry-mass response ratio.

Three shoot strata covered 20 pairs from seven distinct reports (**Table 2**). Fe-amount response relative to dry-mass response was +3.0% for AMF (95% CI −52.0–120.9%; five pairs; $q = 0.884$), +31.6% for bacteria (1.9–70.1%; six pairs; $P = 0.044$; $q = 0.132$) and −6.4% for other fungi (−51.3–80.1%; nine pairs; $q = 0.884$). The bacterial estimate retained $q < 0.05$ in all 15 ordinary Hartung–Knapp correlation scenarios and in none under the modified method. Figure exclusion or the strict reporting subset left two studies.

Thirty condition-matched soil–plant links came from three reports and reused 17 distinct soil effects (**Online Resource 1, Fig. S2**). They combined different soil assays, plant endpoints and interventions and were described individually.

Context models had limited support for explaining response variation

The unified medium test yielded $P = 0.236$; the all-organ field/controlled-setting test yielded P = 0.493. All 181 comparisons in the three-organ core were from controlled experiments. The duration model included 147 comparisons from 28 clusters: each doubling of contact duration corresponded to a response-ratio change of +4.0% (95% CI −18.3–32.4%; $P = 0.714$). The Strategy II/I response-ratio contrast was 1.084 (0.803–1.463; $P = 0.517$); Strategy II in this core represented wheat from five studies. Multiple-target inocula gave a response-ratio contrast of 1.144 relative to single-target inocula (0.886–1.477; 179 comparisons, 33 clusters; $P = 0.236$). None of these exploratory tests identified a clear difference (**Online Resource 1, Table S2**).

Other context variables were limited by independent-study coverage or category overlap. The compatible pH subset contained 53 comparisons from 14 studies but had focal df = 2.47. Explicitly non-sterilized soil came from one study, and the initial Fe-status comparison had df = 3.71. Application-route categories overlapped across microbial classes through only one bacterial substrate-inoculation study. Matched SOC and soil-organic-matter data covered three and six studies, respectively, and were retained separately (**Online Resource 1, Table S2**).

Across the 248 comparable all-organ comparisons, the sample-size predictor had a slope of 0.060 lnRR (95% CI −0.581 to 0.701; $P = 0.840$). The publication-year slope was 0.017 lnRR per decade (−0.192 to 0.226; $P = 0.865$). Joint adjustment gave $P = 0.921$ and $P = 0.919$, respectively **(Fig. 4)**.

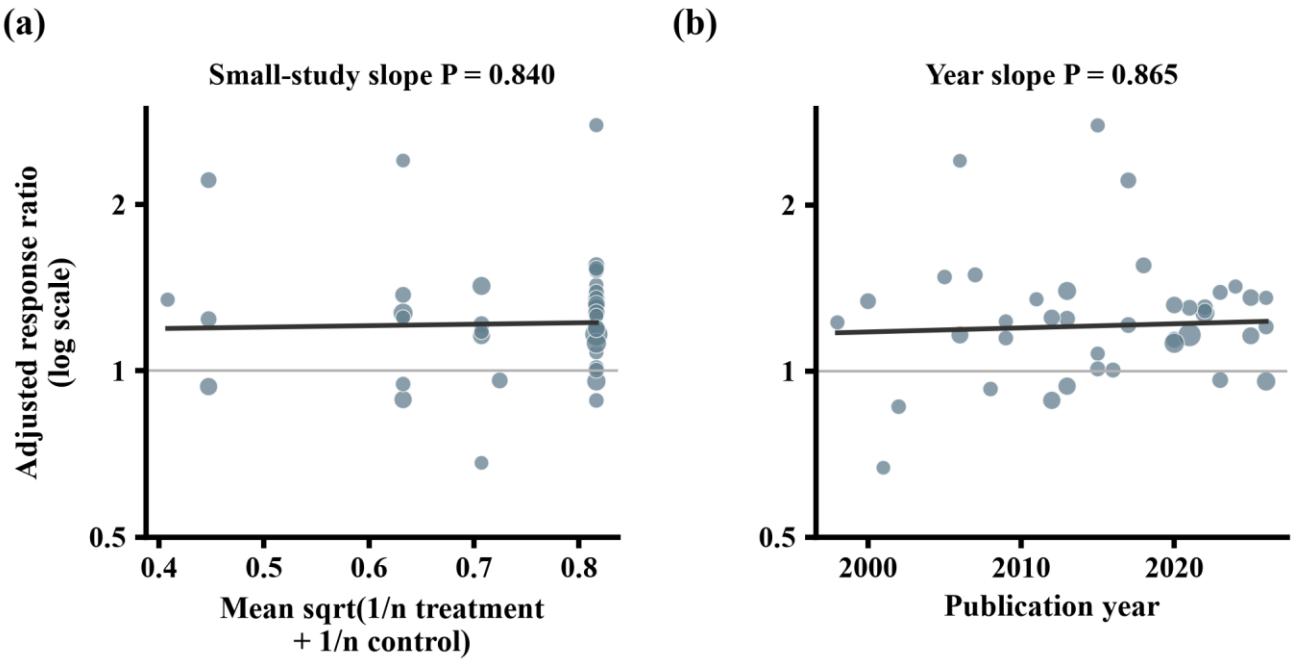


Fig. 4 Study-level displays of sample-size and publication-year diagnostics. Points are equal-within-cluster averages adjusted for non-target fixed terms in the corresponding all-organ model; point area increases with the number of comparisons. Lines display the model intercept and target slope. The regressions and CR2 tests used all 248 comparisons from 40 clusters with their dependence structure, rather than independent regression on the displayed means. Panels show the effective-sample-size predictor (a) and publication year (b). Adjusted response ratios are displayed on a logarithmic scale; diagnostic slopes are reported in lnRR units in the text.

Siderophore attribution was less direct than evidence of microbial Fe responses

Within the 67 reports with reported uncertainty, 36 contained no direct siderophore test, 16 reported traits or biosynthetic potential, three tested crude preparations, nine tested isolated or defined materials and three included targeted functional-loss tests. None combined targeted loss with specific rescue of the relevant plant Fe outcome (**Fig. 5a**). At comparison level, 286 of 533 had no directly attributable siderophore-specific evidence, 156 accompanied trait evidence, 23 involved crude materials and 68 involved isolated or defined materials. The loss tests gave contrasting results. Lurthy et al. (2020) found similar pea Fe-status responses with the producing and deficient treatments. Mališić et al. (2026) found reduced rescue of Arabidopsis Fe deficiency at circumneutral pH but not a requirement for the same pathway under acidic conditions. Wang et al. (2024) reported that a siderophore-deficient comparator failed to reproduce the peanut Fe-nutrition and biomass benefits of its parent. The latter two tests include Fe-status or active-Fe outcomes and support the report-level classification rather than a pooled total-Fe loss effect; the peanut comparison also does not isolate a

single siderophore.

Reporting assessments for the same 67 reports covered all seven domains. Allocation was explicitly reported in 31 reports, unclear in 34, partially reported in one and conflicting in one. Experimental units were clear in 60, clarified from the source in one and of concern in six. Treatment and control backgrounds were matched in all 67 reports. Numerical sources comprised reported values in 37, digitized figures in 22 and specified concerns in eight. Missing samples were unclear in 66 reports and of concern in one, and measurement blinding and selective outcome reporting were unclear in all 67. Unclear ratings indicate insufficient reporting rather than confirmed bias.

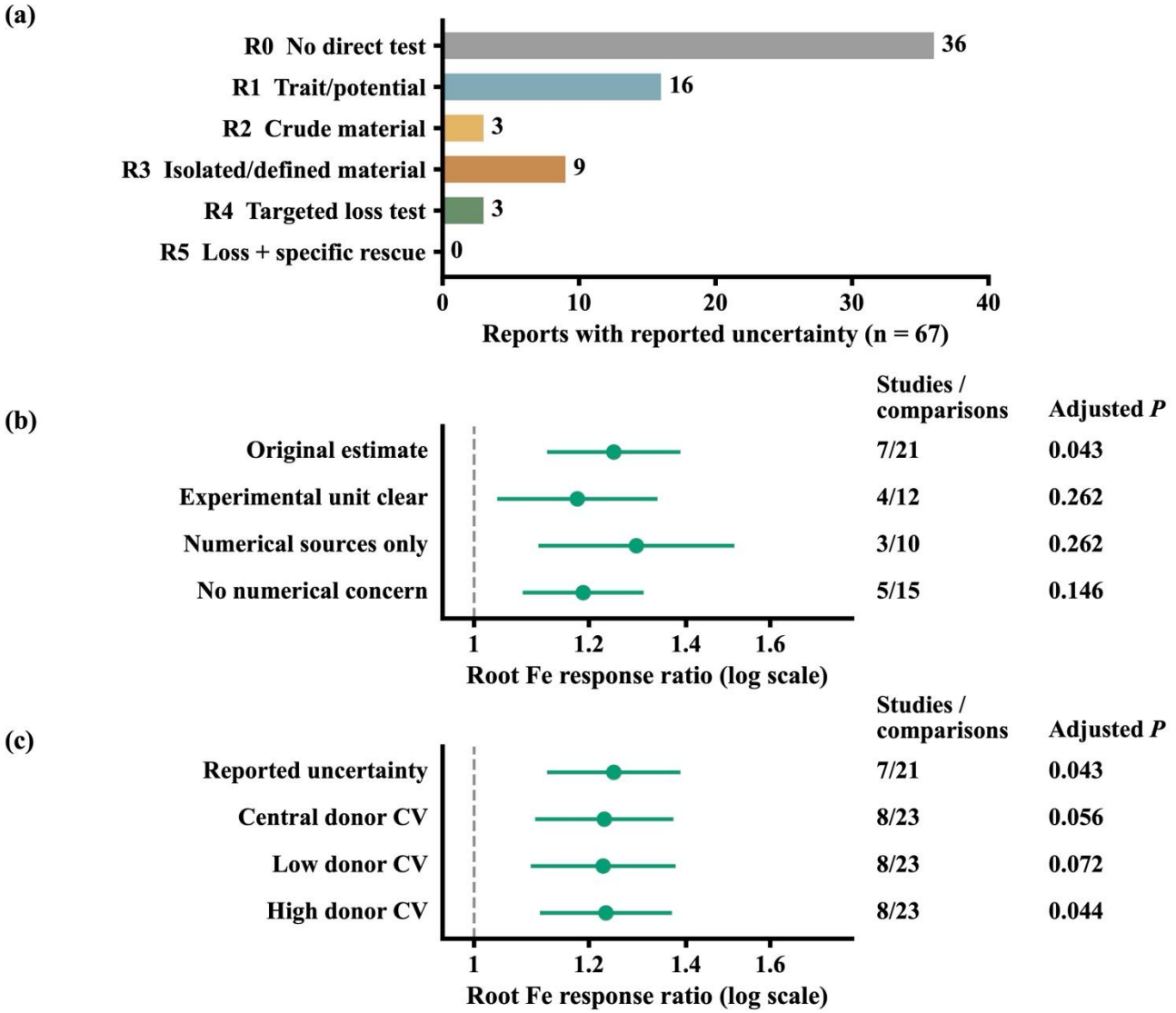


Fig. 5 Siderophore evidence and root-response sensitivity. (a) Report-level evidence categories within the 67 reports with reported uncertainty. (b) Bacterial root Fe concentration under selected reporting-quality restrictions. (c) The same stratum with two additional comparisons from one CV-only report, using central, low and high donor-CV scenarios. Points and lines are estimates and unadjusted CR2 95% intervals. K/k denotes clusters/comparisons; q19 retains the original 19-test outcome family in

each scenario. Low/high refer to donor-CV bootstrap limits, not to treatment-effect confidence limits. The five CV-only reports are separate from the evidence profile in panel a. Panels b and c show response ratios on a logarithmic scale

Quality and CV sensitivities retained the direction of bacterial root enrichment

For the bacterial root-concentration stratum, leave-one-cluster-out estimates ranged from +21.2% to +28.2%. Clear-unit, numerical-source and no-specific-numerical-concern subsets yielded +17.8%, +29.4% and +18.9%, respectively; their unadjusted intervals were above zero, with q values of 0.262, 0.262 and 0.146. Allocation reporting and the combined strict restriction left fewer than three clusters (**Fig. 5b**).

The CV extension comprised 40 comparisons from five reports (El-Ghandour et al. 1995; Mohamed and Ibrahim 2011; Asadollahzade et al. 2018; Lozano-González et al. 2024; Unnikrishnan and Binitha 2024; full citations in the **Appendix of Online Resource 1**). It increased the three-organ concentration dataset to 195 comparisons from 37 clusters and the all-organ dataset to 264 comparisons from 43 clusters. The standardized three-organ mean was +15.7% (95% CI 6.8–25.3%; $P = 0.00074$) with the central donor CV and was +15.7% in all three donor scenarios (**Fig. 2a**). Bacterial root concentration was +23.0% (95% CI 10.5–36.8%; eight clusters, 23 comparisons; $P = 0.00295$). Its original-family q was 0.056 in the central-CV scenario and ranged from 0.044 to 0.072 across low and high scenarios (**Fig. 5c**).

Discussion

Microbial contributions to tissue Fe enrichment across plant-soil interactions

The approximately 14% increase in tissue Fe concentration indicates that microbial activity can influence the Fe supply reaching plant tissues across diverse experimental systems. This is relevant because plant Fe nutrition is often constrained by the accessibility of soil Fe rather than its total abundance. As discussed by (Vélez-Bermúdez and Schmidt 2023), acquisition from alkaline substrates depends on the interaction between root uptake machinery, Fe-mobilizing compounds and the surrounding soil environment. The positive average response observed here supports a nutritional role for microbial processes within this plant–soil interface, extending evidence from individual experiments to a broader set of microbial interventions.

Similar average responses among bacteria, AMF and other fungi may arise through different physiological routes. (Gu et al. 2026b) describe several ways in which microbial siderophores can contribute to plant Fe acquisition, including interactions with established root uptake pathways and direct access to Fe–siderophore complexes. Microbial effects can also operate through stimulation of the host's own acquisition machinery. In red clover, Jin et al. (2006) linked rhizobial enhancement of Fe acquisition to increased root ferric-reductase activity and auxin production, although the tested rhizobia did not produce detectable siderophores under the assay conditions. These examples help explain why broad microbial categories need not produce clearly separated concentration responses: distinct processes can converge on a similar tissue-level outcome. The group comparison therefore provides a basis for considering multiple routes to Fe enrichment rather than ranking microbial groups by presumed mechanism.

The nutritional interpretation of this enrichment depends on its relationship with growth. Earlier syntheses examined AMF effects on micronutrient concentrations (Lehmann and Rillig 2015) and growth responses to siderophore-producing bacteria (Zhang et al. 2023). Connecting these endpoints within the same organ and experiment makes it possible to distinguish enrichment accompanied by greater biomass from concentration changes associated with altered growth. Our paired evidence shows that increased Fe concentration can coexist with increased organ biomass, while also revealing divergent responses. For plant–soil research, the significance is that microbial interventions can be evaluated through their combined effects on tissue enrichment, plant growth and accumulated Fe, providing a more informative basis for assessing nutritional benefits than any single endpoint.

Joint concentration and growth responses clarify the value of tissue enrichment

The most frequent joint-response category combined higher tissue Fe concentration with greater organ dry mass: 25 comparisons from 11 reports, representing 46.8% of the study-balanced distribution. Thus, the positive concentration response can occur alongside growth rather than simply reflecting smaller plants. Opposing responses were also present. Seven comparisons combined greater dry mass with lower concentration, a pattern consistent with growth dilution (Jarrell and Beverly 1981), whereas three combined higher concentration with lower dry mass. Measuring concentration and biomass together separates these outcomes and provides a stronger basis for assessing plant Fe nutrition.

Direct Fe-amount evidence adds the corresponding accumulated pool. Fe-amount responses

covaried positively with dry-mass responses, and the live-inoculation slope was close to one. Because these quantities are linked, the association describes coordinated responses rather than a growth-mediated fraction of Fe acquisition. Individual experiments also illustrate contrasting outcomes: (Sevillano-Caño et al. 2024) reported increased cucumber shoot dry mass and Fe accumulation under some calcareous-soil conditions following yeast inoculation, whereas (García-López et al. 2013) found decreases in both over part of the Fe-supply range. The aligned concentration, biomass and accumulated-pool measurements reveal which type of response occurred.

The bacterial shoot comparison suggested an Fe-accumulation gain exceeding growth, but it rested on three independent study means and was sensitive to the small-sample method. The modified Hartung–Knapp result makes this a useful hypothesis for confirmation rather than a secure average advantage (Röver et al. 2015). Evidence for harvested Fe was also thin: the corpus included two grain Fe-amount comparisons from one report, yet no compatible grain Fe amount–dry-mass pair entered the matched synthesis. Harvest enrichment, yield and dietary Fe bioavailability therefore require their own aligned measurements.

Root and soil Fe pools require a physiological connection to plant supply

Roots are an important acquisition interface and a storage compartment. A larger root Fe pool can contain potentially useful reserves: (Zhang et al. 1991) demonstrated subsequent shoot supply from an apoplastic reserve in wheat, and (Bienfait et al. 1985) described the generation and mobilization of root free-space Fe pools. Under other conditions, apoplastic deposition can accompany root growth arrest (Fang et al. 2024). The root concentration response can thus reflect processes with different consequences for the plant.

Zhu et al. (2025) linked microbial effects on host signalling with root apoplastic Fe reutilization in tomato under Fe limitation, illustrating a route in which mobilizing an existing reserve matters as much as enlarging it. Our root–shoot contrasts did not resolve a preferential organ response, and the seven reports supporting the bacterial root stratum provided limited corresponding Fe-amount and cleaning evidence. Future reports should distinguish ordinary washing, assessment of surface-associated Fe and quantification of apoplastic reserves, and connect these procedures with the relevant shoot or harvested-organ response.

Soil extraction addresses a related supply question at a different scale. DTPA-extractable Fe can

change through dissolution, ligand exchange or redistribution among soil pools, while microbial immobilization and plant uptake occur simultaneously. Thirty matched soil–plant links from three reports were insufficiently uniform to estimate a common transfer relationship. For soil science, the useful implication is that a changed extractable pool should be paired with measured plant Fe accumulation under the same treatment, rather than used as a stand-alone proxy for plant acquisition.

Siderophore evidence should follow the treatment and comparator

Siderophores remain plausible mediators because they bind Fe and alter access to mineral and chelated pools. Their consequences depend on chemical identity, recognition and competition among organisms (Crowley et al. 1991; Schalk 2025). The contrasting chelate-use experiments in barley and oat illustrate this specificity (Römheld and Marschner 1986; Crowley et al. 1988), while recent reviews place it within a wider set of plant–microbe interactions (Gu et al. 2026a, b).

Microbial efficacy and siderophore contribution are complementary questions. In red clover, enhanced Fe acquisition after rhizobial inoculation accompanied ferric-reduction and auxin responses despite the absence of a detectable siderophore signal in the reported assay (Jin et al. 2006). In pea, responses to Fe–pyoverdine materials differed among materials and cultivars (Lurthy et al. 2020). These examples show why a microbial treatment, its culture filtrate and an isolated ligand should retain their separate identities in a synthesis.

The evidence profile made that distinction explicit: most comparisons with reported uncertainty lacked direct treatment-specific siderophore attribution, and only three of the corresponding reports included targeted loss tests. None met the combined loss-and-specific-rescue definition for the relevant plant Fe outcome. The appropriate mechanistic conclusion is therefore that siderophore contribution remains less directly tested than microbial effects on Fe measurements. Equal-Fe source replacement, ligand addition and live inoculation each answer a different question; maintaining those comparators helps connect a proposed mechanism with the actual nutritional response.

Coverage and uncertainty guide agricultural interpretation

Fe availability depends on pH, buffering, redox conditions, ligand turnover and carbon supply, while host Fe status and root development shape acquisition (Marschner 2011; Kobayashi and

Nishizawa 2012; Malisic et al. 2026). AMF add variation in colonization and symbiotic transfer (Kikuchi et al. 2014; Sha et al. 2019; Singh et al. 2025). Our context audit exposed uneven experimental coverage rather than a stable ranking of favourable conditions. Duration and single- versus multiple-target inocula did not show clear associations; host-strategy contrasts were dominated by wheat, and application route was closely aligned with microbial class. Carbon descriptors and explicitly non-sterilized soils were particularly sparse. Broader coverage within comparable experimental designs will be more informative than further subdivision of these data.

Sample-size and publication-year diagnostics showed no clear association with concentration responses after adjustment for organ and microbial group. CV expansion retained a positive overall concentration response. The 22 field comparisons from six reports covered different endpoints and interventions, while grain Fe amount came from one report. The strongest current evidence therefore concerns organ-level enrichment and its relation to biomass under controlled conditions; harvested-organ Fe output remains the next agricultural endpoint to establish.

The main limitations are the uneven representation of organs and experimental conditions, graph-derived data in part of the corpus, and restricted coverage of matched outcomes. The review was not prospectively registered, and the context analyses were exploratory. The concentration–growth categories describe treatment means, with sensitivity analyses addressing response bands and uncertainty coverage.

For evaluating agricultural Fe nutrition, the most informative design aligns tissue concentration, organ dry mass and Fe amount within the same experimental unit and harvest. Soil assays and root-cleaning records clarify the source and location of measured Fe, while harvested-organ Fe and yield connect the response to crop nutritional output. **Figure 6** brings these measurements together: microbial effects are best evaluated through the joint plant response and its connection to the soil Fe supply.

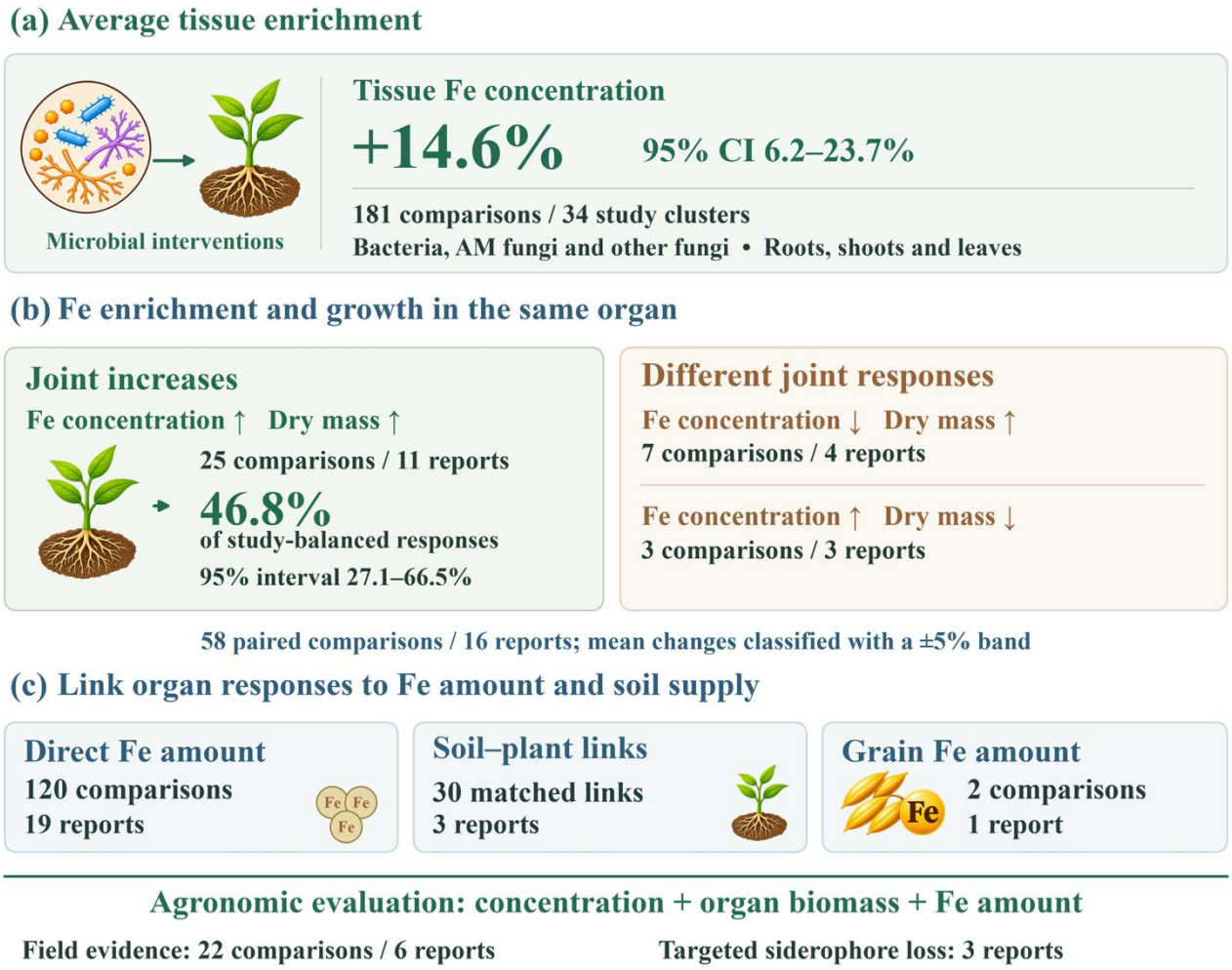


Fig. 6 Evidence connecting tissue Fe enrichment with organ growth, accumulated Fe and agricultural outcomes. The upper panel summarizes the unified concentration response. The central panel shows directly measured concentration–dry-mass pairs, with joint increases defined as more than 5% in both means and percentages calculated with equal study weights. The lower panel places these results alongside direct Fe-amount, soil–plant and harvested-organ evidence. Dataset counts refer to overlapping subsets of the reported-uncertainty corpus; they are not summed.

Agricultural implications

The agricultural value of microbial effects on Fe nutrition lies in whether tissue enrichment accompanies sustained crop growth and greater Fe accumulation in the harvested organ. The positive average concentration response identified here establishes microbial activity as a relevant component of plant Fe nutrition. The matched evidence further shows that enrichment can occur alongside increased biomass. At the same time, greater biomass sometimes coincided with lower Fe concentration, indicating that concentration alone can give an incomplete assessment of the plant

response. Agricultural evaluation should therefore consider tissue Fe concentration, organ biomass and Fe amount together, with emphasis on the organ harvested for food or feed.

This joint assessment is particularly important when connecting changes in soil Fe availability with crop nutritional output. An increase in extractable soil Fe identifies a change in an operationally defined soil pool, whereas plant Fe accumulation shows whether that change is accompanied by a larger plant Fe pool. Measurements made under the same treatment and harvest conditions can connect these two responses. For grain crops, pairing grain Fe concentration with grain yield would establish whether enrichment, yield maintenance and increased Fe removal in the harvested product occur together. Such evidence would bring microbial Fe research closer to the outcomes relevant to crop production and nutritional quality.

Field validation is the next priority for translating the observed tissue responses into agricultural understanding. The current field evidence spans relatively few reports, and direct grain Fe-amount measurements are particularly scarce. Comparisons across sites should retain information on rooting-soil pH, baseline Fe availability, fertilizer management and crop identity, while evaluating the same plant endpoints. These measurements would help establish where the positive responses observed under controlled conditions persist during crop production. An outcome-based approach would provide a stronger basis for assessing whether microbial contributions to soil Fe mobilization translate into improved crop growth and harvested Fe output.

Conclusions

Microbial inoculation increased tissue Fe concentration by approximately 14% across comparable root, shoot and leaf measurements. In matched experiments, enrichment frequently coincided with increased organ biomass, while other comparisons showed concentration dilution or enrichment during growth restriction. Joint measurement of concentration, biomass and Fe accumulation therefore provides a more informative assessment of microbial contributions to plant Fe nutrition than concentration alone. Connecting these organ-level responses with harvested-organ Fe and treatment-specific siderophore evidence is the next step towards agricultural interpretation.

Funding

This work was supported by National Natural Science Foundation of China (Grant No. 3267180650).

Data availability

The data supporting the findings of this study are provided in the Supplementary Data (Online Resource 2), including group-level data extracted from the original publications, source references, experimental characteristics and study eligibility decisions.

Conflict of interest statement

The authors declare no conflict of interest in this study.

References

Benjamini Y, Hochberg Y (1995) Controlling the False Discovery Rate: A Practical and Powerful Approach to Multiple Testing. Journal of the Royal Statistical Society: Series B (Methodological) 57:289–300. https://doi.org/https://doi.org/10.1111/j.2517-6161.1995.tb02031.x

Bienfait HF, van den Briel W, Mesland-Mul NT (1985) Free Space Iron Pools in Roots: Generation and Mobilization. Plant Physiol 78:596–600. https://doi.org/10.1104/pp.78.3.596

Briat JF, Dubos C, Gaymard F (2015) Iron nutrition, biomass production, and plant product quality. Trends Plant Sci 20:33–40. https://doi.org/10.1016/j.tplants.2014.07.005

Chu Q (2026) Handing off iron in plants: from uptake pathways to intracellular chaperones for biofortification. Ann Bot mcag355. https://doi.org/10.1093/aob/mcag355

Chu Q, Li D, Sha Z, He P (2026) Toward Iron-Biofortified Rice: Integrating BRUTUS-Family Regulation and Iron Chaperone Biology. Rice. https://doi.org/10.1186/s12284-026-00953-1

Chu Q, Sha Z, Maruyama H, et al (2019) Metabolic reprogramming in nodules, roots, and leaves of symbiotic soybean in response to iron deficiency. Plant Cell Environ. https://doi.org/10.1111/pce.13608

Colombo C, Palumbo G, He J-Z, et al (2014) Review on iron availability in soil: interaction of Fe minerals, plants, and microbes. J Soils Sediments 14:538–548. https://doi.org/10.1007/s11368-013-0814-z

Connorton JM, Balk J, Rodríguez-Celma J (2017) Iron homeostasis in plants-a brief overview. Metallomics 9:813–823. https://doi.org/10.1039/c7mt00136c

Crowley DE, Reid CPP, Szaniszlo PJ (1988) Utilization of Microbial Siderophores in Iron Acquisition by Oat . Plant Physiol 87:680–685. https://doi.org/10.1104/pp.87.3.680

Crowley DE, Wang YC, Reid CPP, Szaniszlo PJ (1991) Mechanisms of iron acquisition from siderophores by microorganisms and plants. Plant Soil 130:179–198. https://doi.org/10.1007/BF00011873

Fang XZ, Xu XL, Ye ZQ, et al (2024) Excessive iron deposition in root apoplast is involved in growth arrest of roots in response to low pH. J Exp Bot 75:3188–3200. https://doi.org/10.1093/jxb/erae074

García-López AM, Avilés M, Delgado A (2013) Iron availability thresholds for the inoculation of cucumber with Trichoderma asperellum T34. Journal of Plant Nutrition and Soil Science 176:867–875. https://doi.org/https://doi.org/10.1002/jpln.201300277

Gu S, Cui D, Shao J, et al (2026a) Siderophores: chemical threads of rhizosphere health. Trends Microbiol xx:1–10. https://doi.org/10.1016/j.tim.2026.09.006

Gu S, Wang N, Zheng Y, et al (2026b) Integrating microbial siderophores into concepts of plant iron nutrition. Nat Plants 12:. https://doi.org/10.1038/s41477-025-02171-x

Hänsch R, Mendel RR (2009) Physiological functions of mineral micronutrients (Cu, Zn, Mn, Fe, Ni, Mo, B, Cl). Curr Opin Plant Biol 12:259–266. https://doi.org/https://doi.org/10.1016/j.pbi.2009.05.006

Ishimaru Y, Suzuki M, Tsukamoto T, et al (2006) Rice plants take up iron as an Fe3+-phytosiderophore and as Fe2+. Plant Journal 45:335–346. https://doi.org/10.1111/j.1365-313X.2005.02624.x

Jarrell WM, Beverly RB (1981) The Dilution Effect in Plant Nutrition Studies. In: Brady NCBT-A in A (ed). Academic Press, pp 197–224

JIN CWEI, HE YUNF, TANG CAIX, et al (2006) Mechanisms of microbially enhanced Fe acquisition in red clover (Trifolium pratense L.). Plant Cell Environ 29:888–897. https://doi.org/https://doi.org/10.1111/j.1365-3040.2005.01468.x

Kikuchi Y, Hijikata N, Yokoyama K, et al (2014) Polyphosphate accumulation is driven by transcriptome alterations that lead to near-synchronous and near-equivalent uptake of inorganic cations in an arbuscular mycorrhizal fungus. New Phytologist 204:638–649. https://doi.org/https://doi.org/10.1111/nph.12937

Kobayashi T, Nishizawa NK (2012) Iron Uptake, Translocation, and Regulation in Higher Plants. Annu Rev Plant Biol 63:131–152. https://doi.org/10.1146/annurev-arplant-042811-105522

Lajeunesse MJ (2011) On the meta-analysis of response ratios for studies with correlated and multi-group designs. Ecology 92:2049–2055. https://doi.org/https://doi.org/10.1890/11-0423.1

Lajeunesse MJ (2015) Bias and correction for the log response ratio in ecological meta-analysis. Ecology 96:2056–2063. https://doi.org/https://doi.org/10.1890/14-2402.1

Lehmann A, Rillig MC (2015) Arbuscular mycorrhizal contribution to copper, manganese and iron nutrient concentrations in crops – A meta-analysis. Soil Biol Biochem 81:147–158. https://doi.org/https://doi.org/10.1016/j.soilbio.2014.11.013

Lemanceau P, Bauer P, Kraemer S, Briat J-F (2009) Iron dynamics in the rhizosphere as a case study for analyzing interactions between soils, plants and microbes. Plant Soil 321:513–535. https://doi.org/10.1007/s11104-009-0039-5

Lindsay WL, Norvell WA (1978) Development of a DTPA Soil Test for Zinc, Iron, Manganese,

and Copper. Soil Science Society of America Journal 42:421–428. https://doi.org/https://doi.org/10.2136/sssaj1978.03615995004200030009x

Lindsay WL, Schwab AP (1982) The chemistry of iron in soils and its availability to plants. J Plant Nutr 5:821–840. https://doi.org/10.1080/01904168209363012

Lurthy T, Cantat C, Jeudy C, et al (2020) Impact of Bacterial Siderophores on Iron Status and Ionome in Pea. Front Plant Sci 11:1–12. https://doi.org/10.3389/fpls.2020.00730

Malisic M, Copeland C, Amrhein A, et al (2026) Arabidopsis uses distinct coumarins and bacterial pathways for pH-adaptive iron acquisition. Cell 189:6829-6846.e9. https://doi.org/10.1016/j.cell.2026.09.030

Marschner P (2011) Marschner's Mineral Nutrition of Higher Plants: Third Edition

Nakagawa S, Lagisz M, Jennions MD, et al (2022) Methods for testing publication bias in ecological and evolutionary meta-analyses. Methods Ecol Evol 13:4–21. https://doi.org/https://doi.org/10.1111/2041-210X.13724

Nakagawa S, Noble DWA, Lagisz M, et al (2023) A robust and readily implementable method for the meta-analysis of response ratios with and without missing standard deviations. Ecol Lett 26:232–244. https://doi.org/https://doi.org/10.1111/ele.14144

Page MJ, McKenzie JE, Bossuyt PM, et al (2021) The PRISMA 2020 statement: an updated guideline for reporting systematic reviews. BMJ 372:. https://doi.org/10.1136/bmj.n71

Rethlefsen ML, Kirtley S, Waffenschmidt S, et al (2021) PRISMA-S: an extension to the PRISMA Statement for Reporting Literature Searches in Systematic Reviews. Syst Rev 10:39. https://doi.org/10.1186/s13643-020-01542-z

Römheld V, Marschner H (1986) Evidence for a Specific Uptake System for Iron Phytosiderophores in Roots of Grasses. Plant Physiol 80:175–180. https://doi.org/10.1104/pp.80.1.175

Röver C, Knapp G, Friede T (2015) Hartung-Knapp-Sidik-Jonkman approach and its modification for random-effects meta-analysis with few studies. BMC Med Res Methodol 15:99. https://doi.org/10.1186/s12874-015-0091-1

Schalk IJ (2025) Bacterial siderophores: diversity, uptake pathways and applications. Nat Rev Microbiol 23:24–40. https://doi.org/10.1038/s41579-024-01090-6

Sevillano-Caño J, García MJ, Córdoba-Galván C, et al (2024) Exploring the Role of Debaryomyces hansenii as Biofertilizer in Iron-Deficient Environments to Enhance Plant Nutrition and Crop Production Sustainability. Int J Mol Sci 25:. https://doi.org/10.3390/ijms25115729

Sha Z, Watanabe T, Chu Q, et al (2019) A Reduced Phosphorus Application Rate Using a Mycorrhizal Plant as the Preceding Crop Maintains Soybean Seeds' Nutritional Quality. J Agric Food Chem. https://doi.org/10.1021/acs.jafc.8b05288

Singh BK, Hu HW, Macdonald CA, Xiong C (2025) Microbiome-facilitated plant nutrient acquisition. Cell Host Microbe 33:869–881. https://doi.org/10.1016/j.chom.2025.05.005

Vélez-Bermúdez IC, Schmidt W (2023) Iron sensing in plants. Front Plant Sci 14:1–7. https://doi.org/10.3389/fpls.2023.1145510

Viechtbauer W (2010) Conducting meta-analyses in R with the metafor. J Stat Softw 36:1–48. https://doi.org/10.18637/jss.v036.i03

Yang X, Li Y, Yun P, et al (2026) Can heavy metal accumulation in crops be mitigated by microbial inoculants? A meta-analysis and machine learning. J Hazard Mater 514:142858. https://doi.org/https://doi.org/10.1016/j.jhazmat.2026.142858

Zhang F, Römheld V, Marschner H (1991) Role of the Root Apoplasm for Iron Acquisition by Wheat Plants . Plant Physiol 97:1302–1305. https://doi.org/10.1104/pp.97.4.1302

Zhang S, Deng Z, Borham A, et al (2023) Significance of Soil Siderophore-Producing Bacteria in Evaluation and Elevation of Crop Yield. Horticulturae 9:1–10. https://doi.org/10.3390/horticulturae9030370

Zhu L, Zhang A, Guo J, et al (2025) Iron limitation-induced endophytic Ammoniphilus assemblage promotes root apoplastic iron remobilization by attenuation of salicylic acid pathways. NPJ Biofilms Microbiomes 11:. https://doi.org/10.1038/s41522-025-00765-z

Supplementary Files

This is a list of supplementary files associated with this preprint. Click to download.

- Supplementalmaterials.docx